

Published in final edited form as:

Cancer Gene Ther. 2010 April ; 17(4): 266–274. doi:10.1038/cgt.2009.71.

Imaging and therapy of experimental schwannomas using HSV amplicon vector-encoding apoptotic protein under Schwann cell promoter

S Prabhakar^{1,2,3}, **GJ Brenner**^{1,4}, **B Sung**^{1,5}, **SM Messerli**^{1,2,3,8}, **J Mao**^{1,5}, **M Sena-Esteves**^{1,2,3}, **A Stemmer-Rachamimov**^{1,6}, **B Tannous**^{1,2,7}, and **XO Breakefield**^{1,2,6,7}

¹Neuroscience Center, Massachusetts General Hospital, Boston, MA, USA

²Department of Neurology, Massachusetts General Hospital, Boston, MA, USA

³Program in Neuroscience, Harvard Medical School, Boston, MA, USA

⁴Department of Anaesthesiology, Massachusetts General Hospital, Boston, MA, USA

⁵Department of Anesthesia and Critical Care, Pain Research Group, Massachusetts General Hospital, Boston, MA, USA

⁶Department of Pathology, Massachusetts General Hospital, Boston, MA, USA

⁷Department of Radiology, Center for Molecular Imaging Research, Massachusetts General Hospital and Harvard Medical School, Boston, MA, USA

Abstract

Schwannomas are benign tumors forming along peripheral nerves that can cause deafness, pain and paralysis. Current treatment involves surgical resection, which can damage associated nerves. To achieve tumor regression without damage to nerve fibers, we generated an HSV amplicon vector in which the apoptosis-inducing enzyme, caspase-1 (ICE), was placed under the Schwann cell-specific P0 promoter. Infection of schwannoma, neuroblastoma and fibroblastic cells in culture with ICE under the P0 promoter showed selective toxicity to schwannoma cells, while ICE under a constitutive promoter was toxic to all cell types. After direct intratumoral injection of the P0-ICE amplicon vector, we achieved marked regression of schwannoma tumors in an experimental xenograft mouse model. Injection of this amplicon vector into the sciatic nerve produced no apparent injury to the associated dorsal root ganglia neurons or myelinated nerve fibers. The P0-ICE amplicon vector provides a potential means of ‘knifeless resection’ of schwannoma tumors by injection of the vector into the tumor with low risk of damage to associated nerve fibers.

Keywords

neurofibromatosis type 2; bioluminescence imaging; caspase-1; virus vectors; tumors

© 2009 Nature Publishing Group All rights reserved

Correspondence: Dr XO Breakefield, Molecular Neurogenetics Unit, Massachusetts General Hospital-East, Building 149, 13th Street, 6th Floor, Charlestown, MA 02129 USA. breakefield@hms.harvard.edu.

⁸Current address: Biocurrents Research Center, Marine Biological Laboratory, Woods Hole, MA 02543 USA.

Conflict of interest

The authors declare no conflict of interest.

Introduction

Clinical problem of schwannomas and current treatment

Schwannomas are benign tumors derived from dedifferentiation and proliferation of Schwann cells, which myelinate peripheral nerves. Tumors that form along the vestibular nerve can lead to hearing loss and along cranial and peripheral nerves to pain and paralysis. An increased frequency of schwannoma tumors are found in the hereditary conditions, NF2^{1,2} and schwannomatosis.³ Currently, these tumors are treated by surgical resection, which is not always complete and can cause nerve damage. However, because these tumors are typically benign, even reduction in volume can be beneficial. Treatment strategies need to focus on reducing the size of schwannomas, while sparing associated nerves.

Experimental models and therapies for schwannomas

Experimental schwannoma models to evaluate therapeutic strategies have included use of a dominant negative mutation in merlin under the Schwann cell-specific P0 promoter in transgenic mice and conditional knockout of the NF2 gene-encoding merlin in mice crossed to transgenic mice with Cre recombinase under the P0 promoter, both of which show spontaneous formation of schwannomas along peripheral nerves.⁴ Other mouse models include subcutaneous implantation of human schwannoma tissue⁵ or human or murine schwannoma cell lines⁶ into immune compromised mice. Experimental therapies being explored include treatment with EGFR antagonists^{2,7} and oncolytic herpes simplex virus vectors.⁵⁻⁷

HSV amplicon vectors for tumor therapy

Amplicons are a DNA-based vector system in which two non-coding elements of HSV—the DNA origin of replication and packaging signal—are used to package plasmid DNA into HSV virions.⁸ These vectors transduce schwannoma cells and other cell types very efficiently.^{5,6,9} Amplicon vectors have been tested extensively for treatment of different experimental tumors by delivering of pro-drug activating enzymes, apoptosis-inducing factors, fusogenic proteins and siRNAs for growth factor receptors (for review).^{10,11} They have the advantages of efficient transduction of many tumor types, good promoter integrity, the ability to target infection to tumor cells selectively,¹² a large transgene capacity and low inherent toxicity.⁸

Current study

Here, we evaluated the ability of an HSV amplicon vector encoding an apoptosis-inducing protein, ICE (HGP0-ICE-*lacZ*), under the Schwann cell-specific P0 promoter to block growth of schwannoma tumors without injury to associated neurons. Tumors were formed by subcutaneous injection of an immortalized human schwannoma cell line¹³ and monitored by caliper measurements and bioluminescence imaging of tumor-associated Fluc expression. Nerve toxicity was evaluated after direct injection of the amplicon vectors into the sciatic nerve followed by immunohistochemical assessment of increased expression of injury-associated proteins, including transcription factor, ATF3 and growth cone-associated protein (GAP-43) in innervating neurons,¹⁴ as well as nerve conduction velocity (CV) and neuropathologic assessment of nerve damage.

Materials and methods

Cell culture

The HEI-193 human schwannoma cell line (from Dr Lim, House Ear Institute) was established from an NF2 schwannoma patient, immortalized with human papilloma virus

E6/E7 genes¹³ and maintained in DMEM with 2 μM forskolin (Calbiochem, San Diego, CA), 14 ng ml⁻¹ recombinant glial growth factor (Sigma, St Louis, MO) and 500mg G418 (Sigma, St. Louis, MO) (Figure 1a). Human neuroblastoma cell line SH-SY5Y (American Type Culture Collection)¹⁵ was grown in DMEM/F12 (1:1) (Gibco BRL, Rockville, MD). 16 293T human embryonic kidney fibroblasts (from Dr David Baltimore, MIT) were grown in DMEM. For all cell types, growth media were supplemented with 10% FBS (Sigma) and 1% penicillin/streptomycin (Cellgro) and cells were maintained at 37 °C in a humidified atmosphere of 5% CO₂ and 95% air.

Vectors

HSV amplicon plasmids were derived from pHGCX,¹⁷ which carries an HSV origin of replication (*oris*) and cleavage/packaging signal (*pac*); an expression cassette for GFP (Clontech, Mountain View, CA) under the HSV immediate early viral promoter, IE4/5 and an MCS downstream of the immediate early CMV promoter. In one version of the amplicon (pHGC-Fluc) sequences encoding Fluc were placed downstream of the CMV promoter.¹⁸ We also generated other versions of this amplicon (pHGPOX) in which the CMV promoter was replaced with the P0 promoter active in Schwann cells (1.1 kb, from Dr Lemke).¹⁹ The CMV promoter in pHGCX was excised using BglII and EcoRI sites in the MCS, and then the P0 promoter was ligated between these sites. cDNAs for ICE-*lacZ*²⁰ or *lacZ* (pVITRO3-GFP/*lacZ*) were cloned into the MCS at the Not I sites to generate pHGPO-ICE-*lacZ* (Figure 2) and pHGPO-*lacZ* vectors. As a control, the ICE-*lacZ* transgene was also cloned into pHGCX to generate pHGC-ICE-*lacZ*. Amplicon vectors were packaged using the helper virus-free system, as described,²¹ which typically generates vector stocks with titers ~ 10⁸ tu ml⁻¹.

Lentivirus vectors were generated using CSCW-IG, a self-inactivating lentiviral vector, which has a CMV promoter controlling expression of both transgene and GFP cDNAs separated by an IRES element.²² The cDNA-encoding Fluc a (pGL3-basic; Promega Madison, WI) and monomeric red fluorescent protein (mCherry, from Dr R.Tsien)²³ were amplified by PCR. Fluc sequences were inserted directly downstream of the CMV promoter at the Nhe I site and mCherry sequences were inserted in place of the GFP cDNA at Bsa I and Sal I sites, generating pCSCW-Fluc-IRES-mCherry. Lentivirus vectors were generated as described with a typical titer of 10⁸–10¹⁰ tu ml⁻¹.²² To confer stable expression of Fluc and mCherry on HEI-193 cells, they were infected with CSCW-Fluc-IRES-mCherry lentivirus at an MOI of 50, which gave > 90% infectability (cell line termed as HEI-193-FC).

WST-1 assay

Viability was assessed using the cell proliferation reagent, WST-1 (Roche Molecular Biochemicals, Penzberg, Germany). Twelve hundred HEI-193, 293T or SH-SY5Y cells were plated into poly-L-lysine-coated 96-well plates and infected in triplicate with HGP0-ICE-*lacZ*, HGP0-*lacZ* or HGC-ICE-*lacZ* amplicon vectors at an MOI of 5 to achieve > 90% infection. After 72 h, media was aspirated off and cells were incubated in 100 μl fresh media containing 10 μl WST-1 reagent for 4 h under culture conditions. The oxidized tetrazolium salt was measured in wells at 420nm using Spectra max Plus 384 spectrophotometer (Molecular Devices Corp., Sunnyvale, CA).

In vivo schwannoma model

For the establishment of schwannoma tumors, 5 \times 10⁶ HEI-193 or HEI-193-FC cells were suspended in 100 μl reduced serum media (Opti-MEM 1, Gibco), mixed with 100 μl of Matrigel (BD Matrigel Matrix HC, BD Biosciences, Bedford, MA) and implanted subcutaneously into one or both flanks of immunodeficient mice (nu/nu, NCI). When tumor

growth was apparent (~ 3–4 days after the injection), tumor volumes were measured twice a week with external calipers with the volume calculated as $(4\pi/3)(\text{width}/2)^2(\text{length}/2)$.²⁴ When the tumors reached a size of 100 mm³ (baseline day 0), the animals were randomly divided into two groups of three animals each per experiment. Tumors were injected at multiple sites with 2×10^7 tu HGP0-ICE-*lacZ* or HGP0-*lacZ* diluted in 0.9% sodium chloride (1:3) (Abbott Laboratories, North Chicago, IL) in a total volume of 120 μl over 5 min on baseline days 6, 9 and 12 for the first experiment (HEI-193 cells; Figure 3) or 7, 10 and 13 for the second experiment (HEI-193-FC cells; Figure 4).

In vivo bioluminescence imaging

Mice bearing HEI-193-FC tumors were anesthetized by i.p. injection of a mixture of ketamine (25 g l⁻¹) and xylazine (5 g l⁻¹) and injected i.p. with 150 mg kg⁻¹ body weight of the Fluc substrate, D-luciferin. Ten minutes after injection, signal was acquired for 10 s or 1 min using a cryogenically cooled, high efficiency CCD camera system (Roper Scientific, Trenton, NJ), as described.²⁵ Conventional white-light surface images were obtained immediately before each photon counting session to provide an anatomical outline of the animal. After data acquisition, post-processing and visualization were performed using CMIR-Image, a custom-written program with image display and analysis suite developed in IDL (Research Systems, Inc., Boulder, CO). Images were displayed as a pseudo-color photon count image, superimposed on a gray-scale anatomic white-light image, allowing assessment of both bioluminescence intensity and its anatomical source. Regions of interest were defined using an automatic intensity contour procedure to identify bioluminescent signals with intensities significantly greater than background. The sum of the photon counts in these regions was then calculated. At the end of the experiment, tumors were removed, post-fixed overnight and sectioned at 20 μm . GFP fluorescence was visualized directly on perfused sections using a fluorescence microscope. Tumors were stained for S100 using polyclonal anti-cow S100 antibody (Dako, Glostrup Denmark, Carpinteria CA) and secondary antibody, as described.²⁶

Evaluation of neuronal toxicity in DRG

HSV amplicon vector-encoding ICE-*lacZ* or *lacZ* under the P0 promoter was injected into the sciatic nerve of adult nude mice (10^7 tu in 1 μl) over an ~ 10s period (6 per group). Seven days post-injection animals were perfused transcardially with 4% paraformaldehyde in PBS under deep anesthesia, as described,⁶ and innervating DRG (L4-6) on same side removed. DRG were post-fixed for 3 h in 4% paraformaldehyde and cryoprotected overnight in PBS/15% sucrose. DRGs were sectioned at 10 μm and treated with blocking buffer (TNB blocking reagent; Perkin Elmer, Boston, MA) and 0.1% Triton X-100 for 1 h, stained with the primary antibody for ATF3 (Santa Cruz Biotechnology, Inc, CA) diluted in the blocking buffer 1:300 or GAP-43 (Chemicon International, Temecula, CA) 1:1000 at 4 °C overnight. After the incubation, the sections were washed three times in PBS and 0.1% Tween 20 (pH 7.6). The secondary antibody, preabsorbed CY3-conjugated goat anti-rabbit (Jackson Laboratories, Inc., West Grove, PA), was used at a dilution of 1:300 in the blocking buffer for 30 min at room temperature, then sections were washed three times in PBS and mounted with fluorescent mounting media (Dako).

Nerve conduction velocity

The CV was measured 3 weeks after injection of vectors (HGP0-*lacZ*, HGP0-ICE-*lacZ*, G47 Δ) or saline, or with no injection into the sciatic nerve fibers. Under pentobarbital anesthesia (50mg kg⁻¹, i.p.), the sciatic nerve of each treated and untreated mouse was exposed on the left gluteal region. Two electrodes of stimulation and recording were located, respectively, at the distal and proximal part of the nerve around 8 mm apart. The stimulatory electrode was connected to the stimulator (Model 2100, A-M Systems, Carlsborg, WA)

through the stimulus isolator (Model 2200, A-M Systems). Intensity and duration of the stimulus were optimized to supramaximal threshold to induce the compound action potential. The recording electrode was connected to the amplifier MultiClamp 700B with digitizer 1322A (Molecular Devices, Union City, CA). The signals of stimulation and action potential were filtered and digitized at 2 and 10 kHz, respectively, and acquired, amplified and analyzed by Clampex 9.1 and Clampfit 8.0.^{27,28} The first and second peaks after the stimulus peak regarded as the action potentials transmitted by A_α, A_β fibers, respectively. The latency time was measured as time difference between the peaks of the stimulus and response. The CV was calculated as $CV=d/t$ (d : distance between the electrodes, t : time between the peaks of stimulus and response). Data were significant statistically if $P < 0.05$ by ANOVA.

Neuropathology of nerve fibers

The sciatic nerves of mice were injected with vectors or saline, or non-injected as for nerve CV studies. Three weeks later, nerves were removed from deeply anesthetized animals (before euthanasia) and placed into Karnovsky's KII solution (2.5% glutaraldehyde, 2% paraformaldehyde, 0.025% calcium chloride in 0.1 M sodium cacodylate buffer, pH 7.4), fixed overnight at 4 °C and stored in cold buffer. Samples were post-fixed in osmium tetroxide, stained *en bloc* with uranyl acetate, dehydrated in graded ethanol solutions, infiltrated with propylene oxide/Epon mixtures, flat embedded in Epon and polymerized overnight at 60 °C. Sections (1 μm) were stained with toluidine blue to highlight myelin.

Results

Infectability of schwannomas with HSV amplicon vector

To evaluate the extent of gene transfer to schwannoma cells in culture and *in vivo*, immortalized human schwannoma HEI-193 cells were infected with an HSV amplicon vector, HGC-Fluc-encoding GFP and Fluc at an MOI of 1. Forty-eight hours later, cells were visualized for GFP fluorescence showing > 95% infectability (Figure 1a). For *in vivo* monitoring of gene transfer, 5×10^6 HEI-193 cells were implanted subcutaneously into both flanks of nude mice. One week later, both tumors were injected with 10^7 tu HGC-Fluc amplicon vector in 15 μl, and 24 h later, mice were imaged for Fluc activity after i.v. injection of D-luciferin and acquiring photon counts for 10 s using a CCD camera. Marked Fluc activity was observed in tumors injected with HGC-Fluc vector (Figure 1b). To confirm the extent of gene transfer, mice were killed 48 h after the vector injection and tumors were removed and stained by double immunofluorescence for the Schwann cell marker, S100 and reporter protein, GFP (Figure 1c and d). The tumor was positive for the S100 as reported earlier⁶ and showed clear foci of GFP-positive cells.

Specificity of P0 promoter for schwannoma cells

To evaluate the specificity of the P0 promoter for schwannoma cells, different human cell types including human embryonic kidney fibroblasts, 293 T, neuroblastoma cells, SH-SY5Y, and schwannoma cells HEI-193 were infected in culture at an MOI of 5 with HSV amplicon vectors encoding the apoptosis-inducing protein ICE fused to *lacZ* (HGPO-ICE-*lacZ*)²⁰ or *lacZ* alone (HGPO-*lacZ*) under the control of the Schwann cell-specific P0 promoter¹⁹ (Figure 2) or ICE-*lacZ* under the control of the immediate early CMV constitutive promoter (HGC-ICE-*lacZ*). Cell viability was assessed at 72 h post-infection by using a WST-1 assay (Figure 3). The viability of 293 T and SH-SY5Y cells was unaffected by transduction with HGPO-ICE-*lacZ*, whereas 80% of HEI-193 cells were killed by this same vector, confirming the specificity of the P0 promoter for schwannoma cells. In addition, transduction with HGPO-*lacZ* did not cause loss of viability of any cell type, whereas transduction with HGC-ICE-*lacZ* reduced the viability of all cell types to about

50% of naive cell values (Figure 3a). The more extensive death of schwannoma cells with ICE-*lacZ* under the P0 as compared with other cell types supports the cell specificity of this promoter, even though the CMV promoter gave higher levels of expression than the P0 promoter in schwannoma cells, as assessed by levels of *lacZ* expression 24 h after infection with HGP0-*lacZ* vs HGC-*lacZ*.

In vivo treatment of schwannoma tumors with P0-ICE-*lacZ* amplicon vector

To evaluate whether the HGP0-ICE-*lacZ* amplicon vector could be used to treat schwannomas *in vivo*, HEI-193 cells were implanted subcutaneously in one flank of nude mice ($n = 6$) and tumor growth was monitored over time by caliper measurements. When tumor reached about 100 mm^3 in volume (6 days after implantation), half the mice received an intratumoral injection of 10^7 tu HGP0-ICE-*lacZ* vector, and the other half received 10^7 tu of HGP0-*lacZ* control vector. Injections were repeated three times at 3-day intervals (days 6, 9 and 12 post-implantation) and tumor size was monitored at 6-day intervals over a 24-day period (Figure 3b). Tumors that received the HGP0-ICE-*lacZ* vector stopped growing, whereas the tumors injected with HGP0-*lacZ* continued to grow, with the treated tumors being $< 1\%$ the size of control tumors on day 24 ($P < 0.02$).

Imaging of schwannoma therapy in vivo

To image the growth and regression of schwannomas *in vivo*, HEI-193 cells were stably transduced with an expression cassette for Fluc using a lentivirus vector and were then implanted subcutaneously (as above). Tumor growth was monitored over time by *in vivo* bioluminescence imaging after i.v. injection of D -luciferin using a CCD camera. At days 7, 10 and 13 post-implantation, one set of mice ($n = 3$) received an intratumoral injection with HGP0-ICE-*lacZ* (10^7 tu) and the other set ($n = 3$) received 10^7 tu of control HGP0-*lacZ* vector, as above. As expected, tumors that received HGP0-ICE-*lacZ* decreased in size by about 80% ($P < 0.002$) by day 5 after the initial injection, whereas control tumors continued to grow (Figure 4). At day 16, the control group had to be killed because of the large size of tumors. Tumors injected with HGP0-ICE-*lacZ* vector started to grow again very slowly by 25 days after the last vector injection.

Evaluation of toxicity of P0-ICE-*lacZ* amplicon vector to neurons in DRG

To evaluate whether injection of the P0-ICE-*lacZ* vector into nerve fibers would elicit a damage response in innervating neurons from the DRG, we injected 10^7 tu in $1 \mu\text{l}$ HGP0-ICE-*lacZ* or HGP0-*lacZ* (over 10 s) into the distal sciatic nerve of nude mice and evaluated neurons in innervating DRG (L4-6) 7 days later by immunofluorescence. These neurons appeared to be slightly stressed by injection of either amplicon or control vector, as indicated by increased staining for ATF3 (Figure 5a and b) and GAP-43 (Figure 5d and e) as compared with neurons from the DRG of a non-injected control animal processed in parallel, but this difference was not significant (Figure 5c and f). Thus, there is no indication of significant toxicity to neurons caused by injection of the P0-ICE-*lacZ* vector into the nerve fiber.

Effect of vectors on the nerve conduction and integrity of nerve fibers

To determine whether vector injection into the sciatic nerve interfered with nerve conduction, the sciatic nerves of mice were injected with HSV amplicon vectors expressing ICE-*lacZ* or *lacZ* under the P0 promoter (10^7 tu in $1 \mu\text{l}$), an oncolytic HSV vector, G47 Δ (10^7 tu in $1 \mu\text{l}$) or as controls, saline or no-injection. Three weeks after vector injection, nerve integrity was assessed by CV measurements. Conduction velocities of A $_{\alpha}$ fibers in groups of HGP0-ICE-*lacZ* ($n = 4$), HGP0-*lacZ* ($n = 3$), G47 Δ ($n = 4$), saline ($n = 2$) and naive ($n = 3$) were 154.71 ± 0.98 , 148.20 ± 9.43 , 154.71 ± 0.98 , 155.56 ± 0.0 and $153.09 \pm$

3.02, respectively, with no statistically significant difference between groups ($P = 0.901$) (Figure 6). Conduction velocities of A β fibers in groups of HGPO-ICE-*lacZ* ($n = 4$), HGPO-*lacZ* ($n = 3$), G47 Δ ($n = 4$), saline ($n = 2$) and naive ($n = 3$) were 63.45 ± 1.71 , 56.54 ± 5.02 , 61.04 ± 1.02 , 60.03 ± 1.86 and 63.26 ± 1.85 , respectively, again with no statistically significant difference among groups ($P = 0.206$). After nerve conduction studies, nerves were removed and sections from three mice per injection were analyzed for nerve density, loss of myelin and remyelination, presence of macrophages and fibroblasts, axonal degeneration and regeneration. Mild edema, rare degenerating axons and a few infiltrative cells were seen in all samples, including saline controls, apparently in response to the injection itself with no additional abnormalities related to vectors.

Discussion

Findings in this study

In this study, we show that it is possible to block growth of an experimental schwannoma by direct injection of an HSV amplicon vector expressing ICE under a Schwann cell-specific promoter, while avoiding injury to associated nerves. The experimental schwannoma tumor model used has the advantage that the cells are of human origin from an NF2 patient¹³ and maintain features of schwannomas, including expression of S100.⁶ These cells have been immortalized, as non-immortalized human schwannoma cells rarely form tumors in experimental animal models and those grow very slowly *in vivo*.⁵ The HSV amplicon vector has the advantages of preserving the integrity of the P0 promoter in a plasmid backbone with efficient delivery to the nuclei of schwannoma cells mediated by the HSV virion and low-to-no intrinsic toxicity. Thus, direct injection of this vector into the schwannoma has the potential to reduce tumor volume without damaging nerves.

Relationship to earlier studies

There are a number of mouse models of schwannoma tumors available to test therapeutic agents. The dominant negative merlin transgenic model has the advantage that it mimics a mutation found in human schwannomas and tumors form spontaneously along peripheral nerves.^{29,30} However, tumors form in a variety of locations over a 12-month period and must be localized by histology³⁰ or magnetic resonance imaging.²⁶ These tumors also grow slowly and at variable rates in the range of 0.1–0.3 mm³ per day.^{26,5} This limits the ability to carry out direct tumor injections and monitor tumor growth responses to treatment. A conditional NF2 knockout mouse line has also been generated,³¹ and forms slow growing Schwann cell hyperplasia/tumors at variable locations when mated with transgenic P0-Cre mice,⁴ as well as meningiomas when mated with transgenic mice expressing Cre recombinase under an arachnoidal cell promoter.³² Subcutaneous implantation of resected human schwannoma tissue (obtained at surgery) in immune compromised mice results in formation of slowly, variably growing tumors (increasing in volume by an average of 2.5-fold over a month or about 7 mm³ per day).^{5,33} In contrast, injection of immortalized HEI-193 schwannoma cells with Matrigel subcutaneously results in reproducible growth of tumors with about a 20-fold increase in tumor volume over 30 days (50–100 mm³ per day; this study),⁶ making this a more amenable model for evaluating therapeutic intervention, albeit these cells are immortalized to promote tumor growth and thus grow more rapidly than other mouse schwannoma models.

Several studies have been undertaken to evaluate the effectiveness of an oncolytic HSV vector in schwannoma tumor models. The oncolytic vector used, G47 Δ , has deletions in the viral genes for ribonucleotide reductase and gamma 34.5, which restrict its replication to proliferating cells, and for ICP47, which provides enhanced viral growth in tumor cells and increases immune response to viral antigens.³⁴ These properties combined with the high

infectability of schwannoma cells with HSV virions makes G47 Δ a promising therapeutic candidate. Direct injection of this mutant virus into spontaneous tumors in NF2 transgenic mice⁵ or implanted human schwannoma tissue and immortalized schwannoma cells⁶ led to marked regression of tumors. Oncolytic HSV viruses and the EGFR antagonist, erlotinib, have also shown therapeutic efficacy in a xenografts model of human malignant peripheral nerve sheath tumors,⁷ with the latter drug showing variable effectiveness in human NF2 schwannomas³⁵ and HEI-193 in *in situ* model.³⁶ Several oncolytic HSV vectors are in clinical trials for cancer,^{37–39} thus, making this a clinically feasible protocol. However, mutant viruses may elicit an inflammatory reaction, which even if minor could be damaging to nerves, and the slow rate of proliferation of schwannomas limits the replication potential of these oncolytic virus vectors.

Potential therapeutic implications

HSV amplicon vectors have a number of advantages for gene therapy including a large payload (typically multiple copies of the transgene/virion and a 150 kb capacity),⁸ regulatable transgene expression through promoters, which are either drug regulated^{40·41} or selectively active in tumors,^{41·42·40·43} with no replicative potential (being lost with cell division), and little-to-no toxicity or elicitation of immune responses.⁸ The P0-ICE amplicon vector used in this study was found to transduce schwannoma cells efficiently, to restrict ICE expression and cell death to schwannoma cells, and to have no apparent toxicity to neurons *in vivo*. Three intratumoral injections of this vector into schwannoma tumors formed from implanted immortalized human schwannoma cells produced a marked regression of these tumors. Given the slow growth of schwannoma tumors in human beings, this vector has the potential to reduced tumor volume without surgical resection, thus reducing the chance of nerve injury. The resumed growth of tumors after amplicon vector injection presumably reflects both the fact that only a fraction of the tumor cells are infected and that amplicon sequences are lost with successive cell divisions. More effective treatment might result from additional vector injections and use of an HSV/EBV hybrid amplicon vector, which replicates episomally and is distributed to daughter cells.⁴⁴ However, the growth of benign schwannomas in patients is slower than that of the immortalized schwannoma cells used in this tumor model, so regrowth should be proportionally slower in patients. This mode of vector therapy would be most appropriate in cases of vestibular schwannoma, which occur on the VII cranial nerve at the junction of the CNS and PNS, with increasing size leading to nerve compression and deafness and with surgical removal sometimes leading to further nerve damage and deafness.

Abbreviations

CCD	charged-coupling device
CMV	cytomegalovirus
CNS	central nervous system
CV	conduction velocity
DRG	dorsal root ganglia
EGFR	epidermal growth factor receptor
FBS	fetal bovine serum
Fluc	firefly luciferase
GFP	green fluorescent protein
HSV	herpes simplex virus type 1

ICE	caspase-1
MCS	multiple cloning site
MOI	multiplicity of infection (tu per cell)
NF2	neurofibromatosis type 2
PBS	phosphate buffered saline
PNS	peripheral nervous system
tu	transducing units

Acknowledgments

We thank Ms. Suzanne McDavitt for skilled editorial assistance. This work was supported by grants from NINDS NS024279, Department of the Army, US Army Research Medical Research and Material Command Award W81XWH-04-1-0237, the P41 RR001395 NCRR grant, the Terrill Family and Texas Neurofibromatosis Foundation.

References

1. Baser ME, Evans DG, Gutmann DH. Neurofibromatosis 2. *Curr Opin Neurol* 2003;16:27–33. [PubMed: 12544854]
2. McClatchey AI. Neurofibromatosis. *Annu Rev Pathol* 2007;2:191–216. [PubMed: 18039098]
3. MacCollin M, Chioocca EA, Evans DG, Friedman JM, Horvitz R, Jaramillo D, et al. Diagnostic criteria for schwannomatosis. *Neurology* 2005;64:1838–1845. [PubMed: 15955931]
4. Gutmann DH, Giovannini M. Mouse models of neurofibromatosis 1 and 2. *Neoplasia* 2002;4:279–290. [PubMed: 12082543]
5. Messerli SM, Prabhakar S, Tang Y, Mahmood U, Weissleder R, Giovannini M, et al. Treatment of schwannomas with an oncolytic HSV recombinant virus in murine models of neurofibromatosis type 2. *Hum Gene Ther* 2006;17:20–30. [PubMed: 16409122]
6. Prabhakar S, Messerli SM, Stemmer-Rachamimov AO, Liu TC, Rabkin S, Martuza R, et al. Treatment of implantable NF2 schwannoma tumor models with oncolytic herpes simplex virus G47Delta. *Cancer Gene Ther* 2007;14:460–467. [PubMed: 17304235]
7. Mahller YY, Vaikunth SS, Currier MA, Miller SJ, Ripberger MC, Hsu YH, et al. Oncolytic HSV and erlotinib inhibit tumor growth and angiogenesis in a novel malignant peripheral nerve sheath tumor xenograft model. *Mol Ther* 2007;15:279–286. [PubMed: 17235305]
8. Oehmig A, Fraefel C, Breakefield XO. Update of herpesvirus amplicon vectors. *Mol Ther* 2004;10:630–643. [PubMed: 15451447]
9. Aboody-Guterman K, Pechan P, Rainov NG, Sena-Esteves M, Jacobs A, Snyder E, et al. Green fluorescent protein as a reporter for retrovirus and helper virus-free HSV-1 amplicon vector-mediated gene transfer into neural cells in culture and *in vivo*. *Neuroreport* 1997;8:3801–3808. [PubMed: 9427374]
10. Grandi, P.; Bein, K.; Hadjipanayis, CG.; Wolfe, D.; Breakefield, XO.; Glorioso, JC. Application of HSV-1 vectors to the treatment of cancer. In: Harrington, D.; Vile, RG.; Panda, H., editors. *Viral Therapy of Cancer*. Vol. Chapter 2. Wiley Publishers; 2008. p. 2.1-2.8.
11. Shah K, Breakefield X. HSV amplicon vectors for cancer therapy. *Curr Gene Ther* 2006;6:361–370. [PubMed: 16787187]
12. Grandi P, Wang S, Schuback D, Krasnykh V, Spear M, Curiel DT, et al. HSV-1 virions engineered for specific binding to cell surface receptors. *Mol Ther* 2004;9:419–427. [PubMed: 15006609]
13. Hung G, Li X, Faudoa R, Xeu Z, Kluwe L, Rhim JS, et al. Establishment and characterization of a schwannoma cell line from a patient with neurofibromatosis 2. *Int J Oncol* 2002;20:475–482. [PubMed: 11836557]

14. Seiffers R, Allchorne AJ, Woolf CJ. The transcription factor ATF-3 promotes neurite outgrowth. *Mol Cell Neurosci* 2006;32:143–154. [PubMed: 16713293]
15. Sadee W, Yu VC, Richards ML, Preis PN, Schwab MR, Brodsky FM, et al. Expression of neurotransmitter receptors and myc protooncogenes in subclones of a human neuroblastoma cell line. *Cancer Res* 1987;47:5207–5212. [PubMed: 3040240]
16. Hewett J, Gonzalez-Agosti C, Slater D, Ziefer P, Li S, Bergeron D, et al. Mutant torsinA, responsible for early-onset torsion dystonia, forms membrane inclusions in cultured neural cells. *Hum Mol Genet* 2000;9:1403–1413. [PubMed: 10814722]
17. Ikeda K, Saeki Y, Gonzalez-Agosti C, Ramesh V, Chiocca EA. Inhibition of NF2-negative and NF2-positive primary human meningioma cell proliferation by overexpression of merlin due to vector-mediated gene transfer. *J Neurosurg* 1999;91:85–92. [PubMed: 10389885]
18. Shah K, Tang Y, Breakefield X, Weissleder R. Real-time imaging of TRAIL-induced apoptosis of glioma tumors in vivo. *Oncogene* 2003;22:6865–6872. [PubMed: 14534533]
19. Brown AM, Lemke G. Multiple regulatory elements control transcription of the peripheral myelin protein zero gene. *J Biol Chem* 1997;272:28939–28947. [PubMed: 9360965]
20. Jung Y, Miura M, Yuan J. Suppression of interleukin-1 beta-converting enzyme-mediated cell death by insulin-like growth factor. *J Biol Chem* 1996;271:5112–5117. [PubMed: 8617790]
21. Saeki, Y.; Breakefield, XO.; Chiocca, EA. Improved HSV-1 amplicon packaging system using ICP27-deleted, oversized HSV-1 BAC DNA. In: Machida, CA., editor. *Viral Vectors for Gene Therapy, Methods and Protocols*. Vol. vol 76. New Jersey: Humana Press; 2003. p. 51-60.
22. Sena-Esteves M, Tebbets JC, Steffens S, Crombleholme T, Flake AW. Optimized large-scale production of high titer lentivirus vector pseudotypes. *J Virol Methods* 2004;122:131–139. [PubMed: 15542136]
23. Rizzo MA, Springer GH, Granada B, Piston DW. An improved cyan fluorescent protein variant useful for FRET. *Nat Biotechnol* 2004;22:445–449. [PubMed: 14990965]
24. Galve-Roperh I, Sanchez C, Cortes ML, del Pulgar TG, Izquierdo M, Guzman M. Anti-tumoral action of cannabinoids: involvement of sustained ceramide accumulation and extracellular signal-regulated kinase activation. *Nat Methods* 2000;6:313–310.
25. Tannous BA, Kim DE, Fernandez JL, Weissleder R, Breakefield XO. Codon-optimized *Gaussia* luciferase cDNA for mammalian gene expression in culture and *in vivo*. *Mol Ther* 2005;11:435–443. [PubMed: 15727940]
26. Messerli SM, Tang Y, Giovannini M, Bronson R, Weissleder R, Breakefield XO. Detection of spontaneous schwannomas by MRI in a transgenic murine model of neurofibromatosis type 2. *Neoplasia* 2002;4:501–509. [PubMed: 12407444]
27. Gold MS, Weinreich D, Kim CS, Wang R, Treanor J, Porreca F, et al. Redistribution of Na(V) 1.8 in uninjured axons enables neuropathic pain. *J Neurosci* 2003;23:158–166. [PubMed: 12514212]
28. Baba H, Doubell JP, Woolf CJ. Peripheral inflammation facilitates Abeta fiber-mediated synaptic input to the substantia gelatinosa of the adult rat spinal cord. *J Neurosci* 1999;19:859–867. [PubMed: 9880605]
29. Deguen B, Mérel P, Giovannini M, Reggio H, Arpin M, et al. Impaired interaction of naturally occurring mutant NF2 protein with actin-based cytoskeleton and membrane. *Hum Mol Genet* 1998;7:217–226. [PubMed: 9425229]
30. Giovannini M, Robanus-Maandag E, Niwa-Kawakita M, van der Valk M, Woodruff JM, Goutebroze L, et al. Schwann cell hyperplasia and tumors in transgenic mice expressing a naturally occurring mutant NF2 protein. *Genes Dev* 1999;13:978–986. [PubMed: 10215625]
31. Giovannini M, Robanus-Maandag E, van der Valk M, Niwa-Kawakita M, Abramowski V, Goutebroze L, et al. Conditional biallelic Nf2 mutation in the mouse promotes manifestations of human neurofibromatosis type 2. *Genes Dev* 2000;14:1617–1630. [PubMed: 10887156]
32. Kalamirides M, Niwa-Kawakita M, Leblais H, Abramowski V, Perricaudet M, Janin A, et al. Nf2 gene inactivation in arachnoidal cells is rate-limiting for meningioma development in the mouse. *Genes Dev* 2002;16:1060–1065. [PubMed: 12000789]
33. Stidham KR, Roberson JB. Human vestibular schwannoma growth in the nude mouse: evaluation of a modified subcutaneous implantation model. *Am J Otol* 1997;18:622–626. [PubMed: 9303159]

34. Todo T, Martuza RL, Rabkin SD, Johnson PA. Oncolytic herpes simplex virus vector with enhanced MHC class I presentation and tumor cell killing. *Proc Natl Acad Sci USA* 2001;98:6396–6401. [PubMed: 11353831]
35. Plotkin SR, Singh MA, O'Donnell CC, Harris GJ, McClatchey AI, Halpin C. Audiologic and radiographic response of NF2-related vestibular schwannoma to erlotinib therapy. *Nat Clin Pract Oncol* 2008;5:487–491. [PubMed: 18560388]
36. Saydam O, Senol O, Tannous BA, Prabhakar S, Stemmer-Rachamimov AO, Breakefield XO, et al. A novel imaging-compatible sciatic nerve schwannoma model. submitted.
37. Markert JM, Medlock MD, Rabkin SD, Gillespie GY, Todo T, Hunter WD, et al. Conditionally replicating herpes simplex virus mutant, G207 for the treatment of malignant glioma: results of a phase I trial. *Gene Ther* 2000;7:867–874. [PubMed: 10845725]
38. Hu JC, Coffin RS, Davis CJ, Graham NJ, Groves N, Guest PJ, et al. A phase I study of OncoVEXGM-CSF, a second-generation oncolytic herpes simplex virus expressing granulocyte macrophage colony-stimulating factor. *Clin Cancer Res* 2006;12:6737–6747. [PubMed: 17121894]
39. Kemeny N, Brown K, Covey A, Kim T, Bhargava A, Brody L, et al. Phase I, open-label, dose-escalating study of a genetically engineered herpes simplex virus, NV1020, in subjects with metastatic colorectal carcinoma to the liver. *Hum Gene Ther* 2006;17:1214–1224. [PubMed: 17107303]
40. Bragg DC, Camp SM, Kaufman CA, Wilbur JD, Boston H, Schuback DE, et al. Perinuclear biogenesis of mutant torsin-A inclusions in cultured cells infected with tetracycline-regulated herpes simplex virus type 1 amplicon vectors. *Neuroscience* 2004;125:651–661. [PubMed: 15099679]
41. Wang GY, Ho IA, Sia KC, Miao L, Hui KM, Lam PY. Engineering an improved cell cycle-regulatable herpes simplex virus type 1 amplicon vector with enhanced transgene expression in proliferating cells yet attenuated activities in resting cells. *Hum Gene Ther* 2007;18:222–231. [PubMed: 17355186]
42. Reinblatt M, Pin RH, Federoff HJ, Fong Y. Utilizing tumor hypoxia to enhance oncolytic viral therapy in colorectal metastases. *Ann Surg* 2004;239:892–899. [PubMed: 15166969]
43. Ho IA, Hui KM, Lam PY. Glioma-specific and cell cycle-regulated herpes simplex virus type 1 amplicon viral vector. *Hum Gene Ther* 2004;15:495–508. [PubMed: 15144579]
44. Wang S, Vos J. A hybrid herpesvirus infectious vector based on Epstein-Barr virus and herpes simplex virus type 1 for gene transfer into human cells *in vitro* and *in vivo*. *J Virol* 1996;70:8422–8430. [PubMed: 8970963]

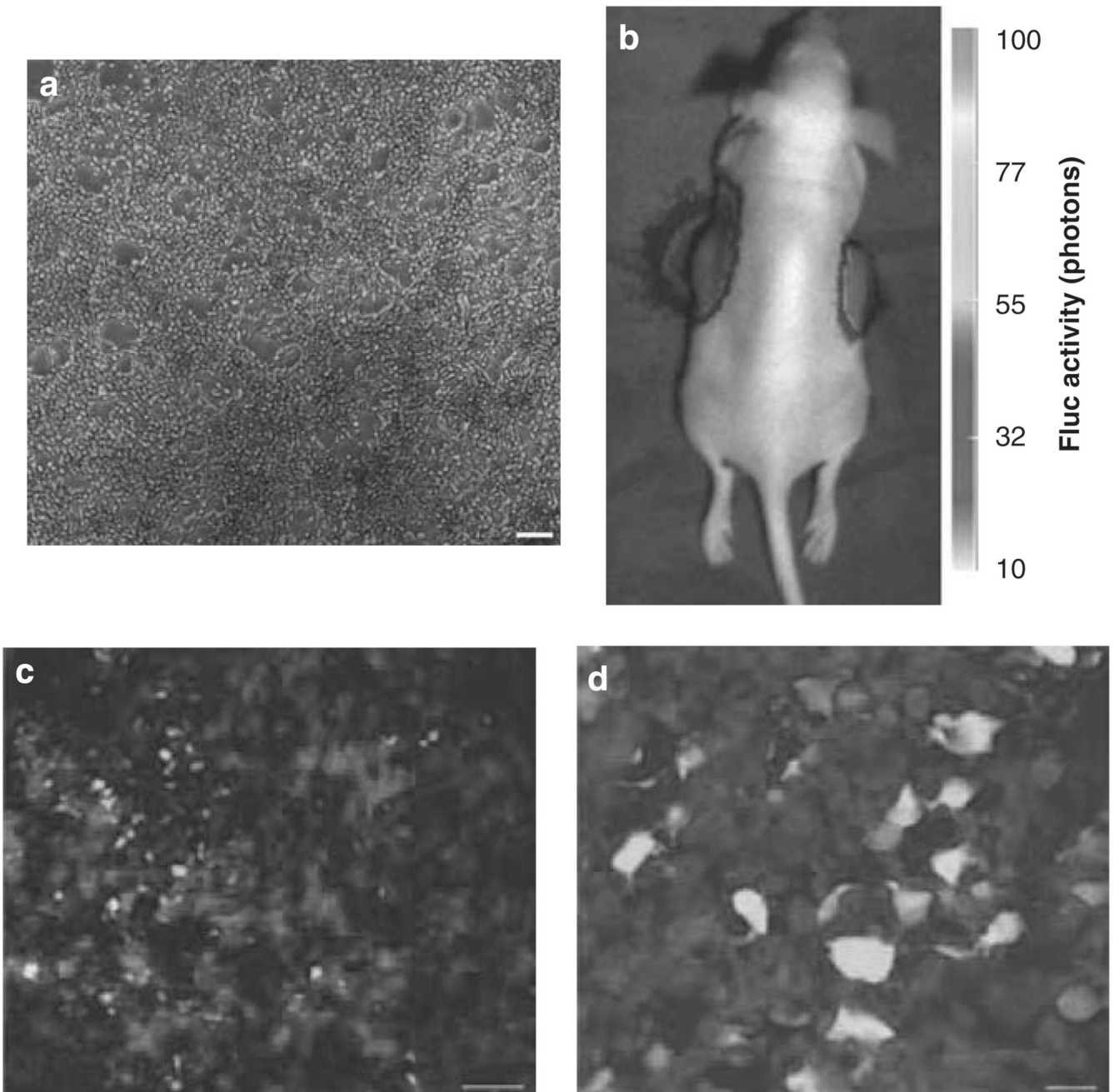


Figure 1. Infectability of schwannomas in culture and *in vivo* with HSV amplicon vector. **(a)** HEI-193 cells were infected with HGC-Fluc HSV amplicon vector. Forty-eight hours later, cells were monitored for GFP fluorescence. **(b)** Five million HEI-193 cells were implanted subcutaneously into both flanks of nude mice. After 1 week, tumors were injected with $15 \mu\text{l}$ 10^7 tu HGC-Fluc vector. Twenty-four hours later, mice were injected with D -luciferin and imaged for Fluc activity using a CCD camera. **(c–d)** Tumors in **(b)** were removed 48 h post-injection and processed for GFP fluorescence (green) and S100 immunofluorescence staining (red). Scale bars: a, $100 \mu\text{m}$; b, $20 \mu\text{m}$. (See online version for color figure)

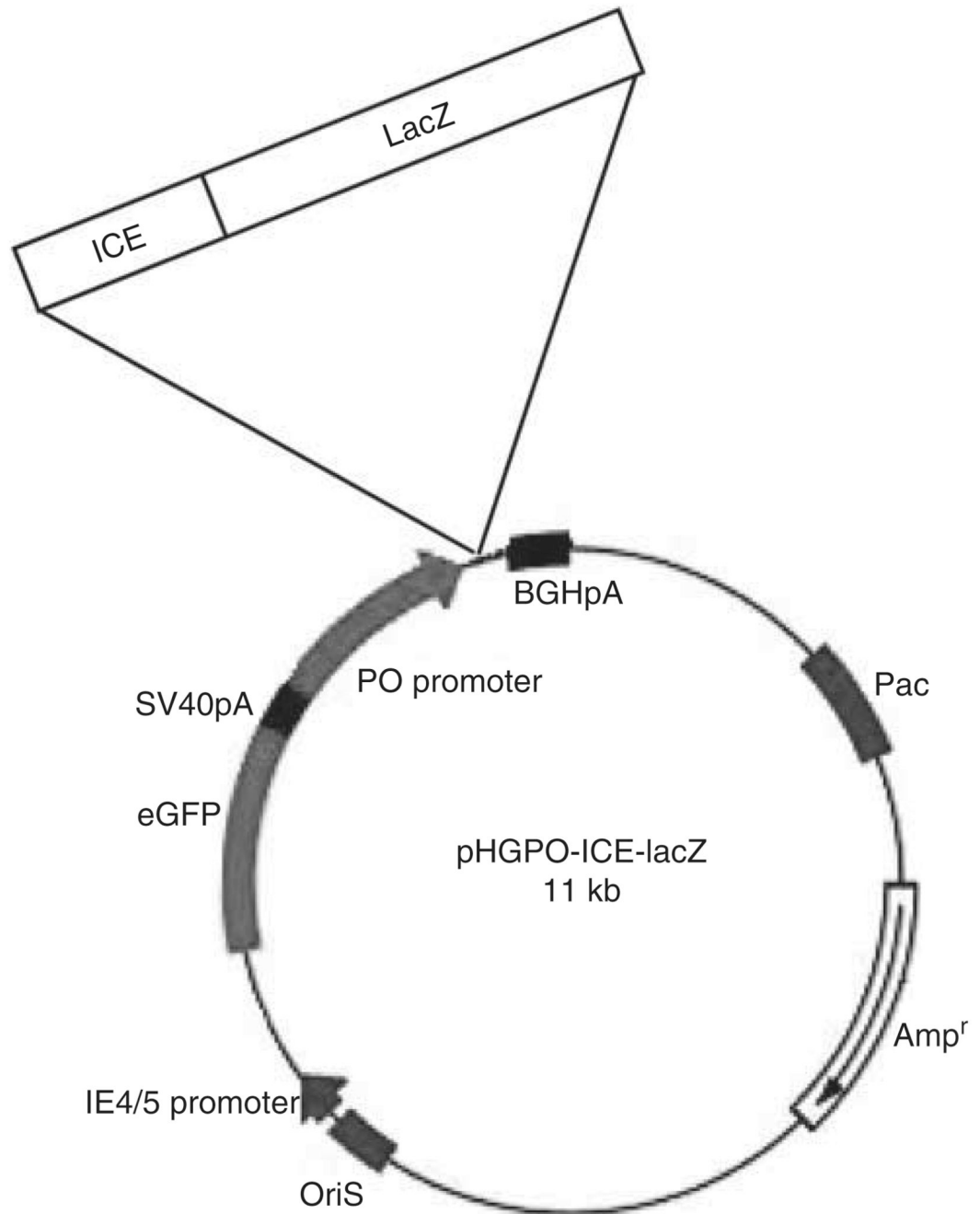


Figure 2. HSV-1 amplicon vectors. Schematic diagram for the HSV amplicon carrying the expression cassette for ICE-*lacZ* under the Schwann cell-specific P0 promoter, with GFP under the HSV immediate early (IE) 4/5 promoter.

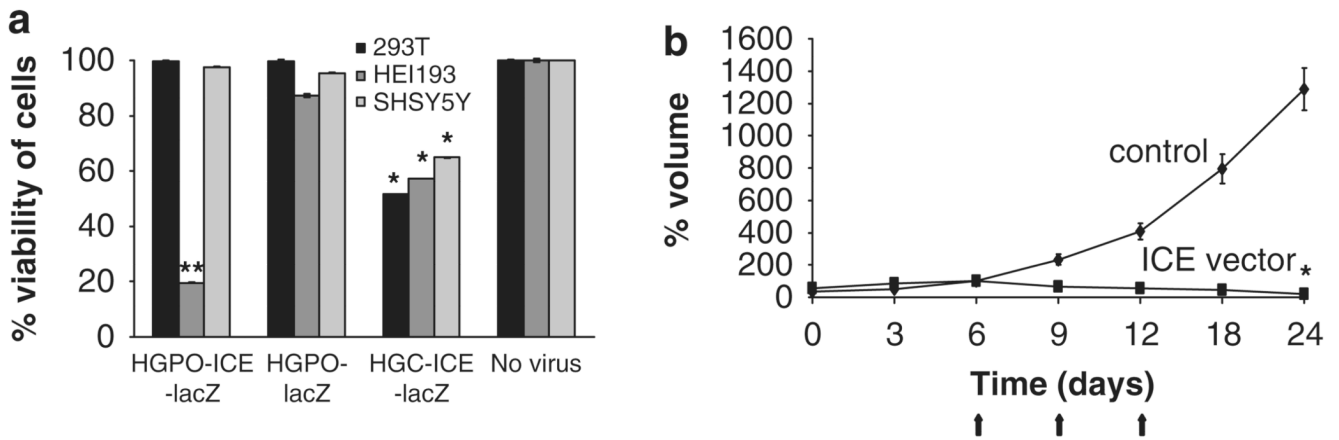
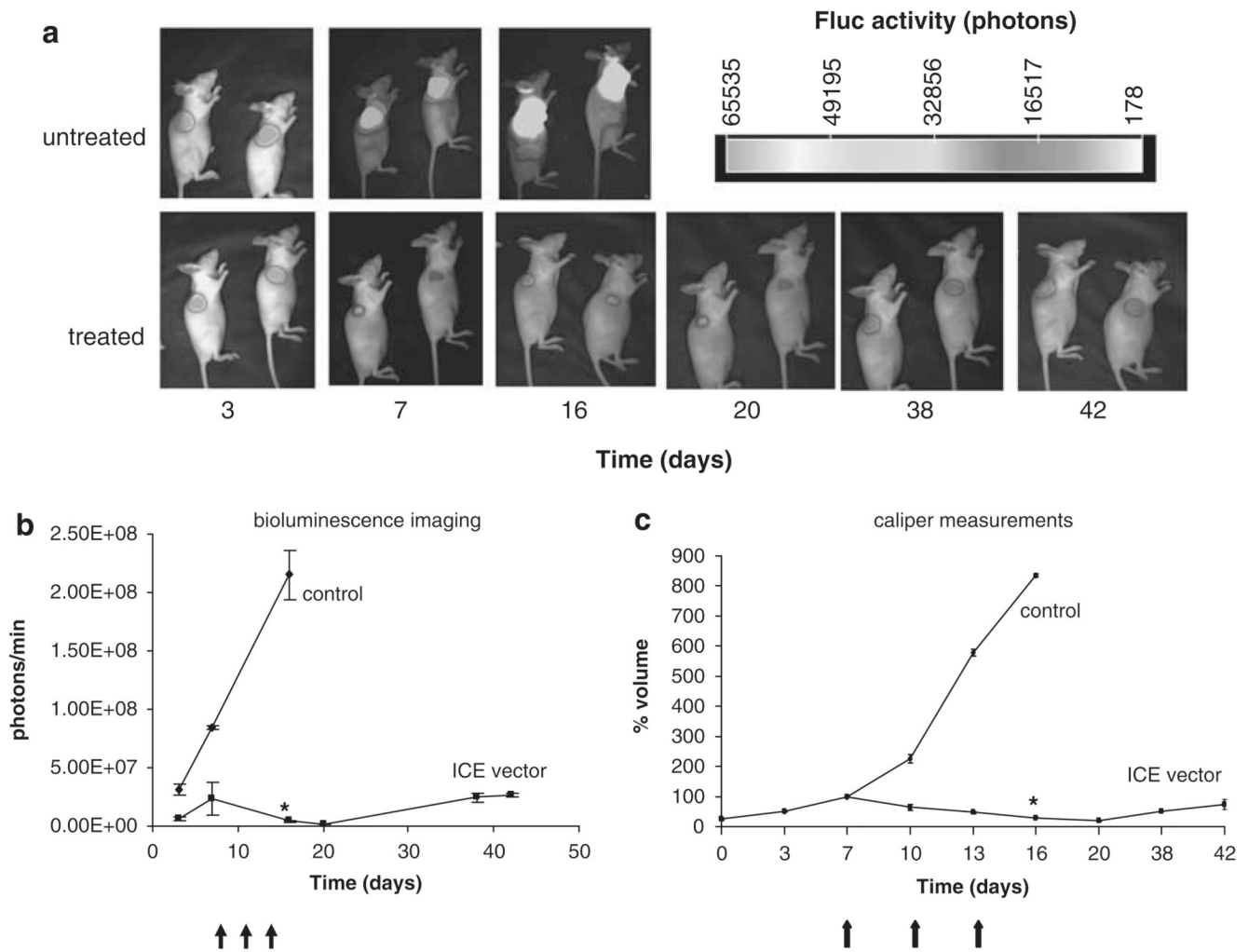


Figure 3.

Specificity of the P0 promoter to schwannoma cells. Cytotoxicity of ICE-*lacZ* under control of P0 promoter was evaluated in culture and *in vivo*. (a) 293 T, HEI-193 and SH-SY5Y human cells were infected with HSV amplicon vectors carrying an expression cassette for either ICE-*lacZ* or *lacZ* under the P0 promoter, or ICE-*lacZ* under the CMV promoter at an MOI of 5. Seventy-two hours post-infection cell viability was evaluated using the WST-1 assay. Levels of significance: HGPO-ICE-*lacZ* in HEI-93 compared with either 293 T or SH-SY5Y cells $**P < 0.005$; HGC-ICE-*lacZ*-treated controls compared with no virus $*P < 0.05$; (b) Five million HEI-193 cells were implanted subcutaneously in nude mice. When tumors reached about 100 mm^3 in volume (day 6; tumor volume set at 100% for each tumor), as calculated by caliper measurements, they were injected with 10^7 tu HGPO-ICE-*lacZ* amplicon vector or HGPO-*lacZ* (control vector) on days 6, 9 and 12 (arrows). Tumor volume was monitored twice weekly with caliper measurements (level of significance between the vector-treated and control tumors at day 24 $*P < 0.05$). Values shown as mean \pm s.d.

**Figure 4.**

Imaging and therapy of schwannomas *in vivo*. Five million HEI-193-FC cells were implanted subcutaneously in nude mice. When tumors reached 100 mm³ in volume (day 7, tumor volume set at 100% volume for each tumor), as calculated by caliper measurements, mice were injected with 10⁷ to HGPO-ICE-*lacZ* or HGPO-*lacZ* vector on days 7, 10 and 13 (arrows). Tumor growth was monitored overtime by both *in vivo* bioluminescence imaging after injection of β -luciferin and acquiring photon counts using a CCD camera with quantitation of signal using CMIR image program (a, b), or by caliper measurements (c). A clear decrease in Fluc activity was observed up to day 20 in tumors injected with HGPO-ICE-*lacZ* amplicon vector consistent with a decrease in tumor size as determined by caliper measurements as opposed to tumors injected with HGPO-*lacZ*, which continued to increase in size (level of significance between untreated and treated tumors on day 16, * $P < 0.002$). Values shown as mean \pm s.d.

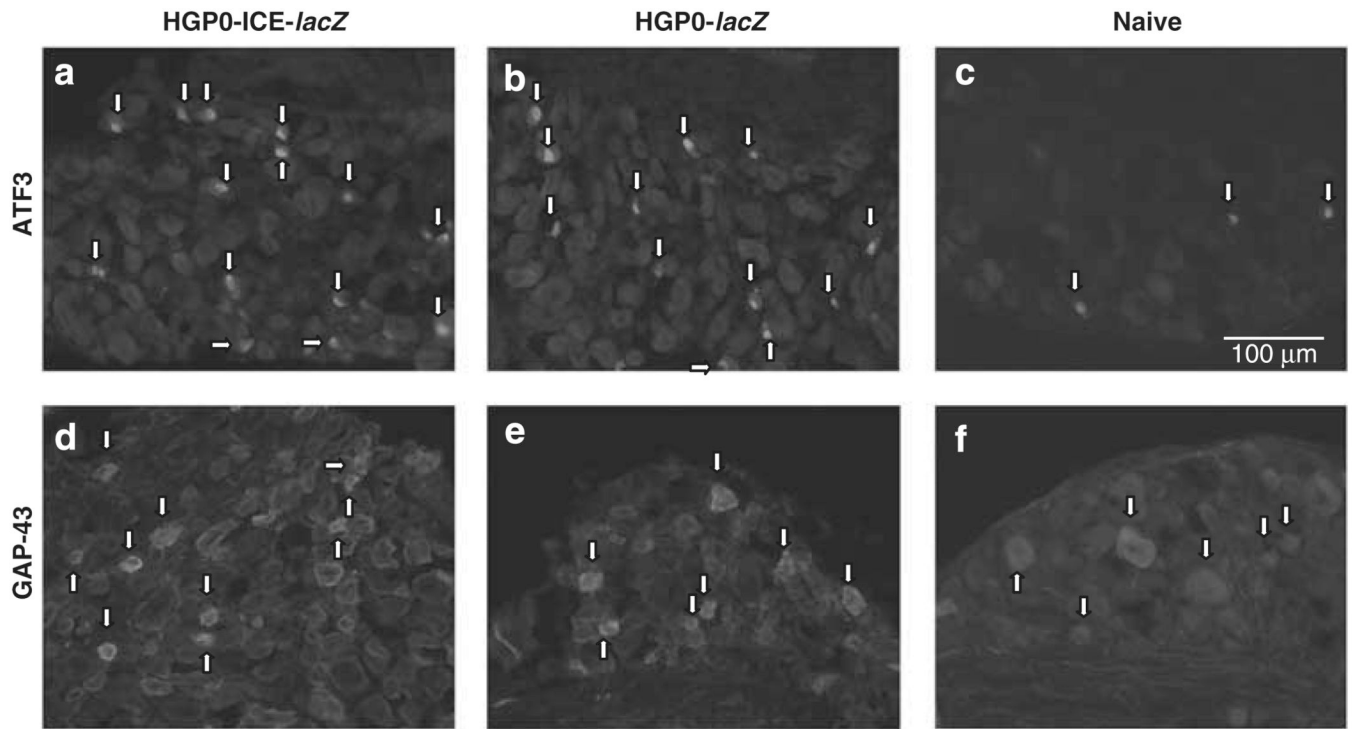


Figure 5.

Vector injection in sciatic nerve causes only mild stress response in innervating neurons. Sciatic nerve was injected with HGP0-ICE*lacZ* (**a, d**) or HGP0-*lacZ* amplicon (**b, e**) vectors and neuronal stress assessed by immunocytochemistry for ATF3 (**a, b**) and GAP-43 (**d, e**) 7 days later. The DRG from an animal receiving no vector injection is shown (**c, f**) for comparison. Examples of cells with upregulated ATF3 and GAP-43 are indicated with arrow heads. Scale bars: 100 μm.

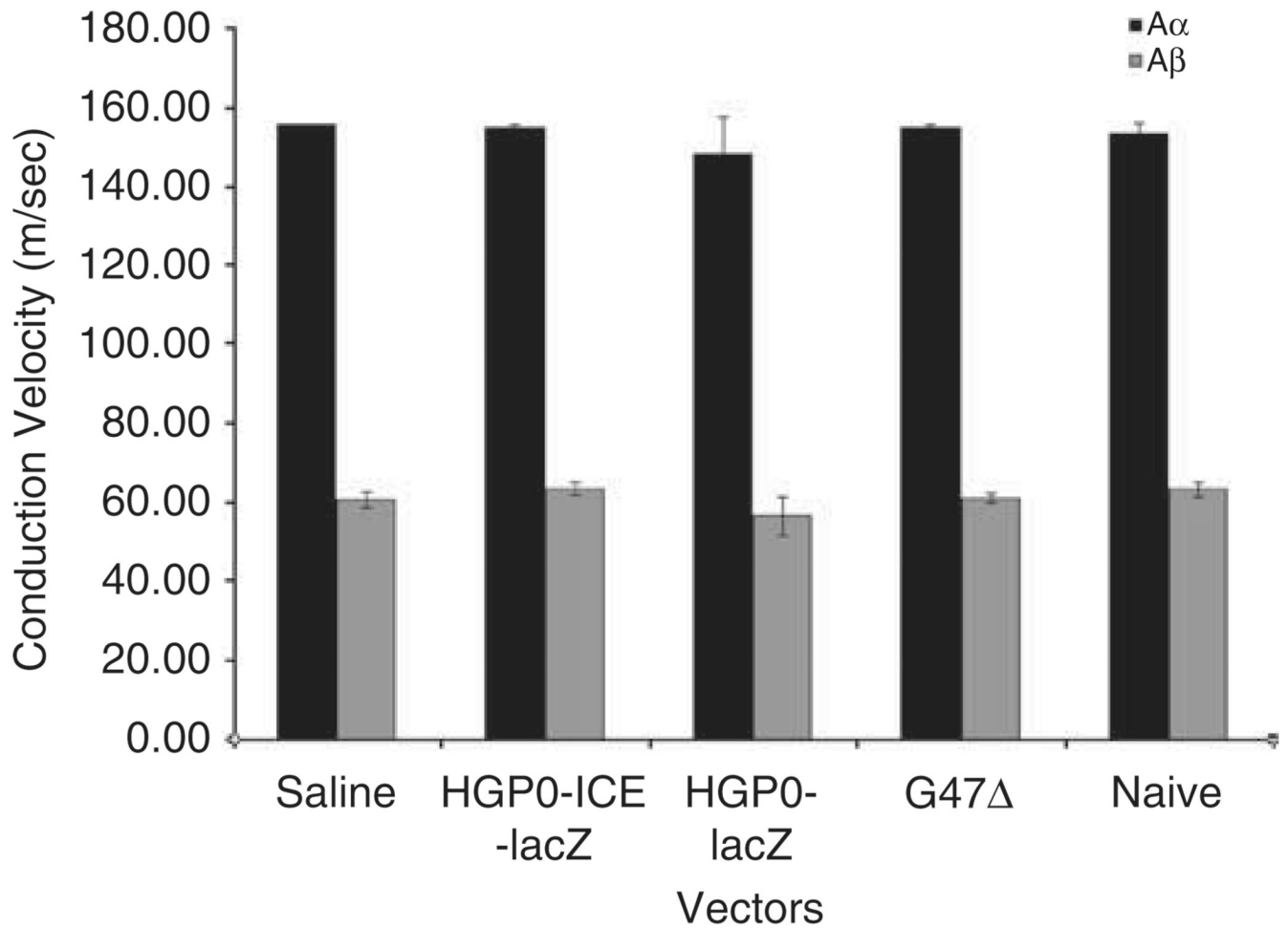


Figure 6. Effect of vector on the CV of the sciatic nerves. Histograms of the CV of A α (black bars) and A β (gray bars) fibers in the sciatic nerve in groups of HGP0-ICE *lacZ* ($n = 4$), HGP0-*lacZ* ($n = 3$), G47 Δ ($n = 4$), saline ($n = 2$) and naive ($n = 3$). There were no statistically significance differences in A α ($P = 0.901$) and A β ($P = 0.206$) between groups.